Detecting cavitation inception in external gear pumps by means of vibro-acoustic measurements

M. Battarra [1], **E. Mucchi** [1]
[1] University of Ferrara, Engineering Deptartment,
Via G. Saragat, 1 - 44122, Ferrara, Italy
e-mail: **mattia.battarra@unife.it**

Abstract
The present work investigates cavitation in external gear machines by means of a dedicated experimental campaign. Four different pump prototypes have been designed and manufactured to perform this research, one of them specifically built up to not be affected by such a phenomenon. Vibro-acoustic measurements performed by a hydrophone and a high-frequency accelerometer are put in comparison with measurements of inlet and outlet pressure ripple, in order to enlighten their capability to follow the development of the phenomenon. Waterfall spectra are investigated and later Root Mean Square (RMS) values of the filtered signals are shown with respect to the cavitation number and compared with efficiency measurements. Results demonstrate that vibro-acoustic measurements associated to a dedicated signal processing procedure represent a powerful tool to detect cavitation inception in gear pumps. In addition, effect of oil temperature is investigated, showing its contribution in spreading the phenomenon on a wider speed range.

1 Introduction

Cavitation detection in fluids machinery represents a central but demanding task in defining the performances of pumps and turbines throughout a wide range of working conditions. Characterizing the machines behavior from the onset of the phenomenon until its full development usually requires a well-assessed measurement procedure and accurate post-processing. One of the first works on this subject pertains to I. S. Pearsall [1], that focused the attention on determining the effects of cavitation by means of acoustic measurements on the performances of various hydraulic machines, such as axial-flow and centrifugal pumps, as well as Francis and Kaplan turbines. Measured data demonstrated that acoustic measurements were more sensitive to the phenomenon inception than efficiency one. These first results have been later supported by more extended experimental campaigns performed on centrifugal pumps [2], demonstrating the effective capability to detect cavitation inception by using hydrophone sensors.

The measurements approach described in [1, 2] has been lately developed and applied to various Kaplan and Francis turbine prototypes [3, 4], underlining the chance to improve the experimental detection with blade-passage frequency demodulation techniques. More recently, different signal processing techniques have been proposed for detecting cavitation inception: M. Čudina demonstrated the possibility to characterize the phenomenon in centrifugal pumps by using audible sound [5]; later, uncertainty of the results was evaluated by the same authors [6]. Adamkowski et al. focused the investigation on monitoring the pump shaft torsional vibrations induced by cavitation erosion [7]. In the same years, Zhaoli et al. presented an assessed method to detect cavitation in pumps with the help of phase demodulated ultrasonic signals [8]. More recently, Azizi et al. developed an algorithm to estimate the severity of the phenomenon in centrifugal pumps [9].

Various other experimental studies on this challenging subject may be found in the literature, however, despite the wide interest shown by the scientific community, a lack of results concerning the detection of cavitation in volumetric machines has been observed by the authors. A small amount of research regards the

effects produced by air release/absorption and oil vaporization in volumetric pumps and motors. Moreover, such works are generally restricted to the numerical approach and focused on the assessment of models for performance prediction. In particular, in [10] Borghi et al. evaluated the influence of cavitation in external gear pumps and motors by proposing a lumped parameter model restricted to the meshing zone, only. More recently, in [11, 12] Zhou et al. presented a lumped parameter approach to evaluate external gear pumps performances under cavitation conditions based on simplified transport equations. The model described in [12] is supported by experimental data referring to the pressure ripple around gears, but no effective data regarding the cavitation detection are provided. Several other works are focused on determining the pump performance taking into account a number of design parameters and working conditions [13, 14, 15, 16], but the cavitation phenomenon is always neglected.

As far as the authors are aware of, the only one experimental work focused on cavitation monitoring in volumetric pumps pertains to Buono et al. [17], that presented an experimental campaign aiming at characterizing the phenomenon in gerotor pumps by means of pressure ripple and vibration measurements. Experimental measurements on cavitation in gear pumps cannot be found in the literature even if this machine type is commonly known to be affected by such a phenomenon [10, 12, 18, 19]. This lack of data might be justified by considering that gear pumps are traditionally driven by electric motors or low speed engines since the requested delivery flow rate is obtained by increasing the pump displacement. Nowadays, in particular in the automotive field, the need to reduce weight and dimensions of the overall system requires to reduce the pump displacement as much as possible and then to guarantee the requested delivery flow rate by increasing the working speed. Based on this brief literature review, the goal of the present work is to characterize cavitation in gear pumps experimentally and define a systematic procedure to detect the inception of the phenomenon with respect to the pump working speed. For this reason, results obtained from the signal processing of different sensors such as accelerometers, hydrophone and pressure pulsation sensors are shown and discussed. Moreover, the analysis of measured data referring to different pumps is supported by measurements of volumetric efficiency and actual detection of various damages produced by cavitation.

The following Section describes the characteristics of the cavitation phenomenon in fluid machines. Section 3 outlines the test setup, concentrating on the description of the test bench adopted to evaluate both pumps efficiency and vibro-acoustic performances, the data acquisition system together with the various transducers installed on the rig and, lastly, the four external gear pumps designed for the experimental campaign and the measurement procedure. Section 4 describes the signal processing techniques applied to measured data, while Section 5 presents the obtained results, with the aim at characterizing gear pumps behavior under cavitating conditions. Finally, last section is devoted to concluding remarks.

2 Cavitation in fluid machinery

The literature survey in Section 1 demonstrates that the cavitation phenomenon in axial/centrifugal pumps and turbines has been widely studied throughout the last five decades. Several experimental campaigns contributed in addressing its characteristics, from a machine performance point of view, as in refs. [1, 2], as well as from a physical point of view, as in ref. [20]. The former approach is based on the evaluation of the machine efficiency with respect to its working condition, which is usually defined in terms of the cavitation number σ:

$$\sigma = \frac{p_{in} - p_{sat}}{0.5\rho u^2} \tag{1}$$

where p_{in} is the mean inlet pressure, p_{sat} is the saturation pressure at the reference oil temperature, ρ is the oil density at the reference temperature and u is the mean flow velocity at the inlet port. As described in ref. [21], the cavitation number is a scaling parameter adopted to extrapolate data from one working condition to another by assuming complete similitude guaranteed by a constant cavitation number itself. However, in practice, σ does not include all the variables influencing the phenomenon, e.g. boundary geometry, absolute pressure, local velocity or pressure drop, and therefore such a parameter is still affected from scale effects.

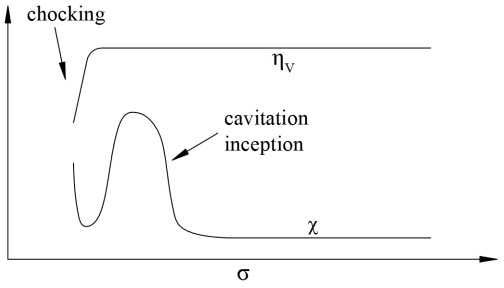

Figure 1: Qualitative trend of volumetric efficiency η_V and generic vibro-acoustic quantity χ with respect to the cavitation number.

Once the cavitation number is assumed as a control parameter, starting from a cavitation-free working condition, by reducing σ the generic turbomachine cross three main regions: the first one coincides with the initial condition, then as the machine approaches the cavitation inception region, small, isolated and localized bubbles start appearing. As σ keeps decreasing, the phenomenon intensifies till the machine enters the fully-developed cavitation region and starts working in chocked conditions.

These considerations explain the results obtained in [1, 2], which demonstrated that efficiency measurements cannot follow the evolution of the phenomenon entirely, since the delivery flow rate starts being influenced by cavitation when the machine enters the fully-developed cavitation region. On the contrary, measurements based on hydrophones, accelerometers, acoustic emission sensors and pressure transducers were shown to be much more sensitive to the phenomenon, being able to detect it from the inception to its complete development. In particular, several experiments demonstrated that vibro-acoustic measured quantities always follow a common trend as the cavitation number is decreased from the free-of-cavitation region till the fully-developed one, as shown in Figure 1. Volumetric efficiency η_V remains unaltered till the chocked condition, when it finally shows a sharp drop; on the contrary, generic vibro-acoustic quantity χ starts increasing as soon as the inception takes place, it reaches a maximum and then suddenly drops down as the phenomenon intensifies. If σ is further decreased, chocking starts appearing and χ starts increasing again.

These results are usually obtained by executing a large number of measurements where σ is gradually decreased by reducing the inlet pressure while the working speed is set as a constant. The practical advantage given by this kind of approach stands in the possibility to fully characterize the phenomenon by simply regulating a valve placed on the inlet side. Moreover, since this kind of machines is typically designed to work at a fixed constant speed while the inlet pressure depends on the installation layout, the proposed approach also gives an accurate representation of the real case.

In order to have a complete overview of the problem, it must be clarified that the necessity to detect cavitation inception comes from a practical reason. Although fully-developed cavitation affects volumetric efficiency seriously, it is proved to be less damaging than the inception condition in terms of wear and erosion. As explained in refs. [21, 22], when cavitation becomes well developed, the flow aggressiveness tends to decrease due to a smaller production of vapor bubbles or weaker implosions. For this reason, detecting cavitation from its inception becomes a crucial task to define the working condition range where the machine can operate safely.

Despite the large amount of specialized literature regarding cavitation on hydraulic machines, similar studies have never been performed for gear pumps. For this reason, a clear description regarding how and where the phenomenon takes place and evolves is not available in the literature. Concurrently, experimental data for correlating cavitation in gear pumps with respect to vibro-acoustic measurements cannot be found. However, by taking advantage of the numerical results in ref. [11] regarding the vapor and air mass fractions evolution around the gears, it is possible to assume a realistic description of its development. Since bubble generation

requires a consistent drop of the local pressure, air release and vaporization must necessarily take place in the meshing zone, when the trapped volume opens to the inlet chamber. Within this context, the oil suddenly flows from a high pressure zone to a low pressure one by means of an extremely small orifice, which causes the flow velocity to increase significantly. Since oil speed sudden increases, a further decrease of the local pressure is produced with the consequent effect of promoting cavitation. Once bubbles are generated, they can either collapse in the suction chamber or be trapped by gear pockets, dragging them into the pressurizing zone. As soon as the pressure inside the pockets increases, bubbles collapse and produce undesired noise, vibration and, potentially, wear.

On the basis of this description, it is clear that both working speed and suction pressure are crucial parameters. If the speed is increased, the oil pressure inside the meshing zone tends to increase as well and therefore the subsequent pressure drop becomes more and more intense. Moreover, the speed increase produces a slight reduction of the mean suction pressure that contributes in intensifying the phenomenon. On the other hand, cavitation can be also induced by decreasing the mean inlet pressure till the bubble generation can take place directly inside the suction chamber. Although the two mechanisms lead to the same final effect of promoting cavitation inside the pump, they cannot be considered equivalent since speed increase and suction pressure reduction have a different influence on the pressure course around the gears. As described by Mucchi et al. in [23, 24], the speed increase produces a consistent reduction of the pump sealing capability; since the pressure increase in the pressurizing zone is delayed, the bubble collapse is also expected to be delayed. The proposed explanation clarifies the reason why cavitation tests in gear pumps for automotive applications should be performed by increasing the working speed rather than reducing the inlet pressure. This kind of pumps are designed to work safely throughout an extended speed range, while the installation layout is fixed; in this way, each specific pump is designed for a specific lubrication system. Therefore, in this framework, the inlet pressure does not actually represent a control parameter of the phenomenon, which appears to be mainly governed by the working speed.

3 Experimental setup

3.1 Test rig description

The test rig adopted to carry out the experimental campaign is shown in Figure 2. The gear pump is installed inside a sealing box that makes it working submerged and driven by a brushless AC motor with speed controller; a torque meter is located along the shaft connecting the pump with the electric motor. The pipeline for the oil supply system is constituted by two branches: one connecting the tank to the sealing box and the other one connecting the pumps outlet chamber to the tank. An automatic servo valve located on the latter branch of the pipeline allows for the fast regulation of the oil delivery pressure. The oil temperature is regulated with an additional pipeline connected to the tank and controlled by a dedicated system, namely the temperature controller. Such a system monitors the oil inside the tank by using a thermocouple and regulates the temperature with a number of electric resistances.

Both pipeline systems described above are equipped with a drainage system, various valves and filters in order to allow for a safe and easy management of the test rig during the measurement procedures. The description of such auxiliary parts of the test rig is neglected being out of the scope of the present work.

3.2 Sensors and data acquisition system

Two different sets of transducers have been adopted to carry out the experimental campaign. As shown in Figure 2, a first set of sensors has been used to control the test rig and monitor the working condition of the pump under examination. In particular, two digital pressure gauges have been placed on the suction and delivery ports, respectively, in order to check the mean inlet and outlet pressure. A Kracht Gear Type Flow

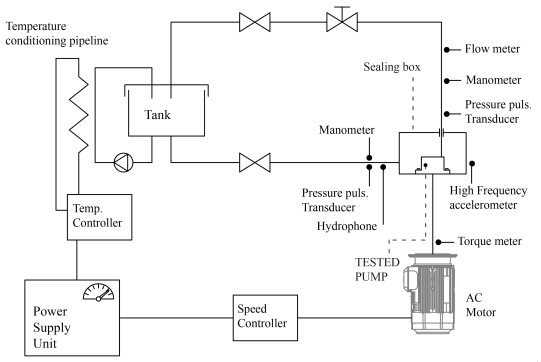

Figure 2: Test rig configuration and sensors disposition adopted for the experimental campaign.

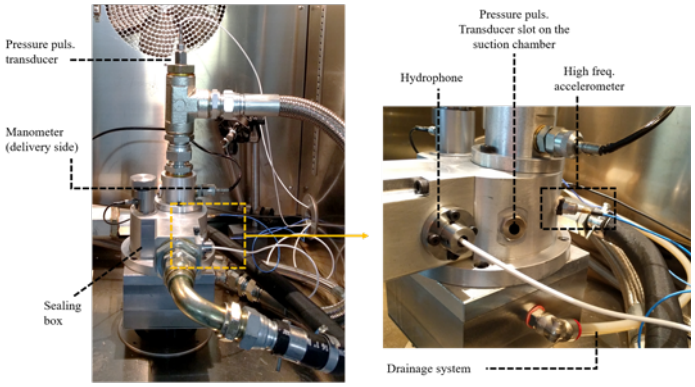

Figure 3: Transducers setup in the real test configuration. As underlined in Section 3.1, the sealing box does not allow for a direct access to the pump casing.

Meter has been used to measure the outlet flow rate, while the instantaneous angular speed can be directly acquired from the tachometer connected to the speed controller of the electric motor.

The second set of sensors has been specifically designed to detect the presence of cavitation by means of vibro-acoustic measurements (see Figure 3). With this purpose, two high frequency piezoelectric transducers (model PCB S102B with resonant frequency above 500kHz) have been place on the suction and delivery ports respectively, in order to measure the pressure ripple generated by the pump. Moreover, a miniature hydrophone (model B&K 8103), located in proximity of the suction chamber and connected to a conditioning amplifier (model B&K Nexus 2692), monitors the acoustic pressure of the oil. Finally, a high-frequency single-axis accelerometer (model PCB 352A60 with resonant frequency above 95kHz) has been located on the sealing box, close to the beginning of the pressurizing zone related to the driving gear. This choice is justified by the fact that while bubbles are generated in the last part of the meshing zone, they are supposed to collapse in the first part of the pressurizing zone. This assumption is supported by direct observation of the wear produced by cavitation on the pump casing. This second set of sensors, together with the signal provided by the tachometer, has been acquired with a LMS Scadas 305 acquisition system and then postprocessed in Matlab environment. In order to capture the signature produced by cavitation phenomena, the sample frequency f_s has been set to the maximum value allowed by the adopted acquisition system, which is equal to 204800Hz.

3.3 Gear pumps type and measurement procedure

Four different gear pump prototypes have been designed and manufactured in order to perform a wide experimental campaign allowing for a satisfactory characterization of the phenomenon. The first prototype, namely Pump A, is constituted by helical gears, with 14 teeth on the driving gear and 9 teeth on the driven one. Since the pump casing is made by steel, no running in process is required and therefore radial clearances between gears and casing are entirely defined by design. The second prototype, namely Pump B, is composed by the same gearpair used for Pump A, but the casing is milled from a single block of aluminum. For this reason, radial clearances are reduced during the design process since the gear pair can mill its own grooves into the casing during the running in process. The third prototype, namely Pump C, is made up by a spur gearpair, with 13 teeth on the driving gear and 10 teeth on the driven one. As described for Pump B, Pump C has an aluminum casing that requires the running in process before the pump can be considered ready to be tested. Finally, the last prototype, namely Pump D, is made by an aluminum casing and helical gears, with 11 teeth and transmission ratio equal to one. All the four prototypes have similar global dimensions and displacement (around $14cm^3/rev$). Pump D has been specifically designed to avoid the presence of cavitation inside the range of working conditions tested. The main design features of the four described prototypes are summarized in Table 3.3.

The four pumps have been tested by following the same measurement procedure: the prototype is installed on the test rig and the servo valve is set to maintain a mean delivery pressure equal to 30bar. The oil temperature is set at 60^oC and kept as a constant by the temperature controller. With these constraints settled up, each pump is tested at different speed values, starting from 800rpm till 6000rpm, with a constant step of 100rpm. The maximum speed is limited by the maximum torque provided by the electric motor. Moreover, experimental tests regarding prototype A have been repeated at 90^oC and 120^oC in order to evaluate the influence of the oil temperature. Tests have been performed without reducing the inlet pressure by regulating a valve in the inlet piping, but the speed increasing solely induces cavitation. Despite this testing procedure is uncommon when evaluating the influence of cavitation in fluid machines, it is a more realistic representation of the phenomenon that may take place in actual gear pump applications, e.g. in the auxiliary systems for automotive applications. These pumps are usually driven by the engine and therefore must properly work throughout a wide speed range; on the contrary, the installation can be designed to minimize pressure losses on the inlet pipeline making this parameter less dominant on the evolution of the phenomenon.

Pump Type	z_1/z_2	**Tooth Type**	**Case Material**	p_{out}
A	$14/9$	Helical	Cast iron	30bar
B	$14/9$	Helical	Aluminum	30bar
C	$13/10$	Spur	Aluminum	30bar
D	$11/11$	Helical	Aluminum	30bar

Table 1: Main design characteristics of the four tested prototypes.

In order to verify the presence/absence of cavitation in each pump prototype, endurance tests have been performed on each gear machine and later the potential presence of wear has been assessed. Endurance tests have been performed for 60 hours at the most severe working condition, which corresponds to a combination of angular speed/delivery pressure equals to 6000rpm/30bar. As expected, wear has not been detected on pump prototype D, while various marks of erosion due to cavitation have been observed on prototype A, B and C. In particular, endurance tests on various samples of pump prototype A had to be stopped before the expected time due to severe wear that compromised the correct machines operation.

4 Post processing

The early detection of cavitation phenomena in hydraulic machines by means of vibrational and acoustic measurements requires the design of specific post processing procedures, typically based on the evaluation

of the demodulated signal at the blade passage frequency [3, 4, 20, 25]. However, the application of these methods in the present study did not provide any valuable result. It is the author's belief that such a negative outcome is linked to the methodology adopted in this study to promote cavitation, which is induced by increasing the working speed of the pump, without modifying any other working condition parameter. This method differs considerably from the classical approach that has been described in the literature since the very first publications, in which cavitation is promoted by the reducing the suction pressure at constant nominal speed. This latter method has the benefit to freeze the dynamics of the machine with respect to the working condition; as a consequence, any change recorded in the machine response can be attributed to the cavitation development. Concurrently, as explained in Section 2, the approach is a well representation of real cases: axial/centrifugal machines are designed to work at fixed nominal speed, but they may encounter different suction pressure values depending on the installation layout. On the contrary, gear pumps are often designed to be installed on a specific layout, e.g. in the automotive field a specific pump is designed for a specific driveline transmission, but they are required to work safely throughout a wide speed range. Within this framework, it is therefore clear that promoting cavitation by increasing the working speed is a more realistic reproduction of the real case, even if the machine dynamics becomes to be influenced by both the working condition and the cavitation development. As a matter of fact, the speed increase causes the amplitude of the harmonics of the mesh frequency, together with their sidebands potentially present, to vary through the considered speed range depending on (i) the dynamics of the gearpair, (ii) the dynamics of the overall pump body and (iii) the fluid-dynamics of the machine. This particular behavior masks the signature of cavitation throughout the low frequency range typically excited by the first $10-15$ harmonics of the mesh frequency.

On the basis of these considerations, the phenomenon has been characterized by using an energetic approach applied to a frequency range less involved by the pump dynamics. The first step of the developed procedure consists of calculating the waterfall diagrams of the acquired signals. Waterfall charts are not determined by performing a Short Time Fourier Transform on a single run up, since they can be directly estimated by piling the data acquired at constant speed and expressed in frequency domain on a single chart. By repeating this procedure for each sensor, a general overview of the pump behavior is obtained and the frequency limit value that bounds the low frequency range can be defined by direct observation of such charts. Moreover, as it will be shown in Section 5, waterfall diagrams allow for a preliminary and qualitative evaluation of the presence of cavitation.

The second step of the post processing procedure starts with filtering the data by using a high-pass filter with cutoff frequency equals to the frequency limit value determined in the previous step. Filtered signals at each working speed are then analyzed by calculating their RMS value and displayed with respect to cavitation number σ [2]. The methodology is able to determine the presence of high frequency cavitation noise, in particular when enlightened by the presence of resonances inside the analyzed frequency range.

5 Results and discussion

In the current section, results obtained from the signal processing procedure described in Section 4 are shown and discussed. Attention is particularly focused on showing the signature caused by the presence of cavitation and the different capability of the four adopted sensors in capturing the phenomenon. Moreover, in order to misleading conclusions, the capability to distinguish the cavitation noise from the structural one is verified by applying the the proposed method to a non-cavitating pump.

In order to better understand the importance of the first step of the post processing procedure, waterfall charts of the signals referred to pumps B and D are reported in Figure 4. The latter is specifically designed to not be affected by cavitation in the analyzed working range conditions. Results, that are displayed in logarithmic scale, have been previously normalized by their minimum value and divided by the reference value $k = 10^{-3}$ (the normalized quantity is indicated with symbol $\tilde{X}$). For each plot, two main regions can be distinguished: the low frequency region, which extends to the 40kHz limit in the currently analyzed pumps, and the high

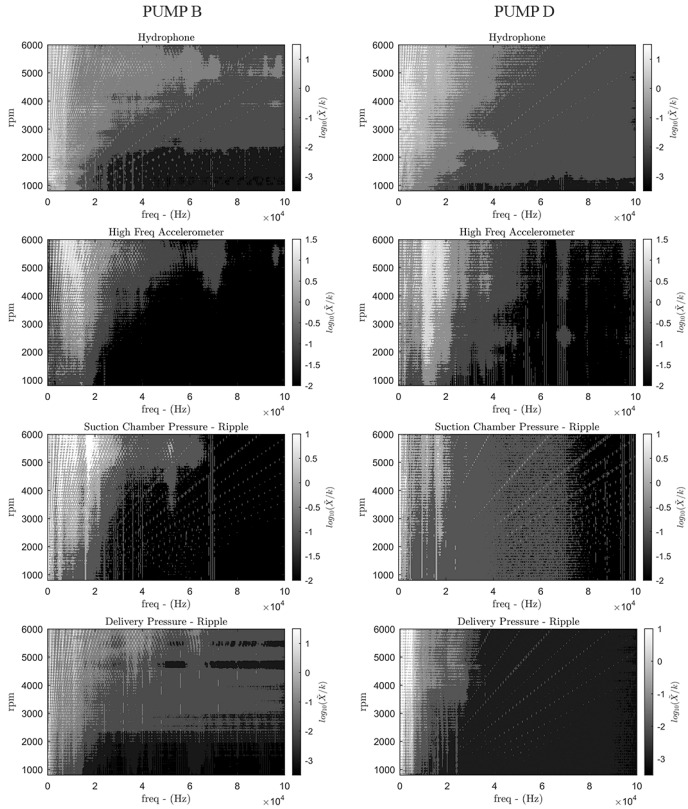

Figure 4: Waterfall plots (in logarithmic scale) of the acquired data referred to pump prototype B, affected by cavitation, and prototype D, not affected by cavitation. In each plot, symbol $\tilde{X}$ refers to the measured quantity normalized by its maximum value.

frequency region, which involves the remaining frequency range. The former region is mainly influenced by the periodic components of the signal, typically harmonics of the angular speed and the mesh frequency. The latter, on the contrary, refers to a frequency range that is usually too high to be crossed by harmonics of the mesh frequency with a relevant amplitude. Concurrently, as also observed in [2, 3, 20], the high frequency range is usually the one characterized by the cavitation signature. Based on these considerations, the waterfall plots become a powerful tool for the determination of the frequency limit that will be used to set the cutoff frequency of the high-pass filter in the following step of the post processing.

Waterfall charts in Figure 4 represent also a valuable tool for a preliminary detection of cavitation. Focusing the attention on the suction chamber pressure ripple, for example, the signals referred to the two pumps show a completely different behavior in the high frequency region. For each arbitrary frequency band within this region, the noncavitating one (prototype D) is characterized by the absence of amplitude gradient along the entire speed range, except for the presence of some high order harmonics of the mesh frequency. On the contrary, the signal referred to the cavitating one (prototype B) outlines the presence of high frequency broadband components between 40 and 70kHz. Such broadband components start being appreciable, in terms of amplitude, qualitatively from 4200rpm, reach a maximum amplitude value at around 5500rpm and then a decrease is observed. The described phenomenon is recognized also in the signals obtained from the other transducers; in particular, hydrophone measurements appear to be the most sensitive, since such a behavior is present throughout the entire bandwidth of the high frequency region.

By following the signal processing procedure defined in Section 4, data referred to pump prototypes B and D have been high-pass filtered at 40kHz and then the RMS value for each transducer at each working speed condition has been calculated (Figure 5). Results are reported together with the measured volumetric

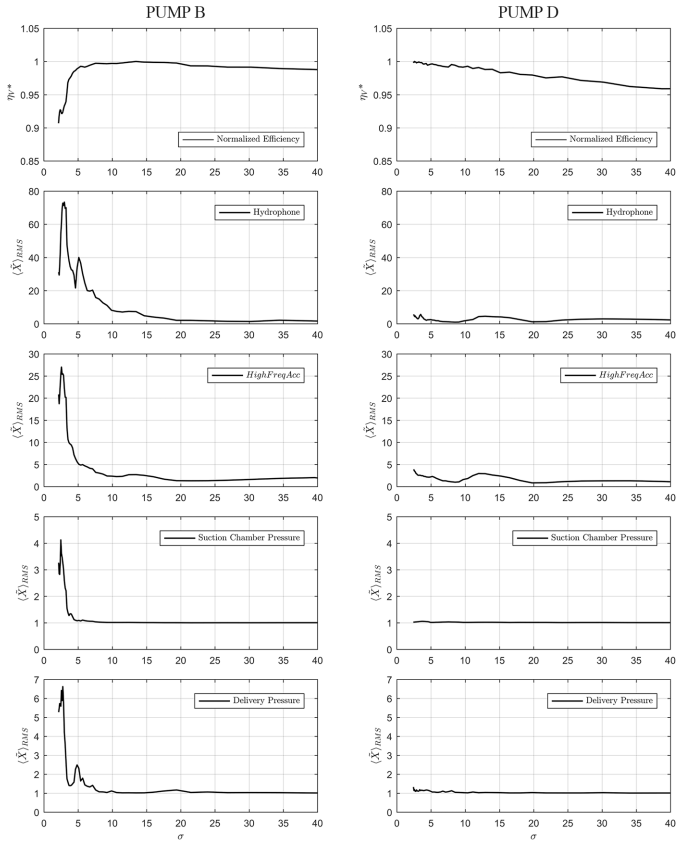

Figure 5: RMS values of the four measured signals and volumetric efficiency as a function of the cavitation number σ, for pump prototypes B and D. In each plot, symbol $\tilde{X}$ refers to the measured quantity normalized by its minimum value, while symbol η_V^* refers to the volumetric efficiency normalized by its maximum value.

efficiency and expressed with respect to the cavitation number σ. For the sake of clarity, measurements performed with hydrophone, accelerometers and pressure transducers are normalized by their respective minimum value. Volumetric efficiency is normalized with respect to its maximum value for confidentiality reasons. As can be appreciated from Figure 5, the efficiency referred to pump B shows the typical sharp drop caused by the presence of intense cavitation; on the contrary, no efficiency reduction is detected for pump D. By focusing the attention on the cavitating one, it is possible to observe that in conformity with the efficiency drop that starts taking place at about $\sigma = 5$, all the four signals show a strong increment of the RMS value. Moreover, as often described in the literature [1, 2, 25, 5], the RMS value reaches a maximum when cavitation is close to the fully developed condition and then starts decreasing. It is therefore clear that intense cavitation phenomena are captured by pressure pulsation measurements as well as acceleration and acoustic measurements. However, since it is well known that incipient cavitation takes place well before the efficiency drop [1, 2, 25], it is interesting to notice that pressure pulsation measurements appear not to be able to detect it. In particular, suction chamber pressure pulsation results to be the least sensitive to the phenomenon since the RMS value begins to increase when the efficiency drop is already developed. On the contrary, both acceleration and acoustic measurements start rising considerably before the efficiency drop, and in particular around $\sigma = 15$. In analogy to the observations made in [25], it is reasonable to assume that incipient cavitation takes place in the range between $\sigma = 10$ and $\sigma = 15$, where pressure pulsation measurements are not affected by a significant variation in their RMS values.

The behavior described by vibration and acoustic measurements can be also appreciated in Figure 6, which reports the results of the post processing applied to acoustic measurements performed on prototype A at three

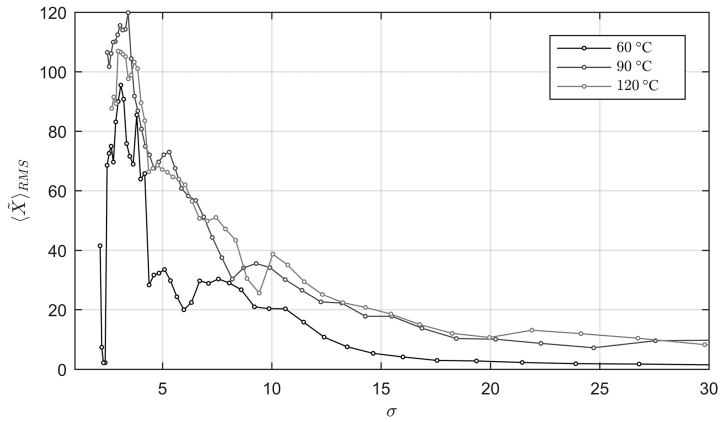

Figure 6: RMS values referred to the hydrophone measurements on pump prototype A at different oil temperature. Symbol $\tilde{X}$ refers to the measured quantity normalized by the minimum value recorded for the 60^oC case, while symbol η_V^* refers to the volumetric efficiency normalized by its maximum value.

different temperature values. The cutoff frequency of the high-pass filter has been set at 45kHz and results have been normalized by the minimum value obtained for the 60^oC case. By focusing the attention on the 60^oC case, it can be noted that the analyzed speed range (from 800rpm to 6000rpm) is able to characterize the entire development of the phenomenon, which starts being detected at $\sigma = 14$. By increasing the speed, i.e. by reducing the cavitation number, RMS value increases and reaches a maximum at $\sigma = 3.10$; after this value, the RMS of the filtered signal shows a sharp drop till the minimum value recorded at $\sigma = 2.38$ and it then starts raising again. Such a particular behavior has been described several times in the literature for rotordynamic machines [1, 2, 25, 5, 26] but no similar data are already available in the literature for positive-displacement machines. Figure 6 allows also for the evaluation of the effect produced by the oil temperature on the cavitation phenomenon. As it can be appreciated, temperature variation does not cause a significant modification of the overall behavior since the maximum of each curve is bounded by $\sigma = 2.97$ and $\sigma = 3.43$. However, since for a given working speed the temperature increasing makes the cavitation number to reduce, measurements performed at 90^oC and 120^oC cannot describe the development of the phenomenon entirely. Practically speaking, the increase of oil temperature spreads the phenomenon on a wider speed range and, in particular, it moves the fully developed cavitation condition at higher speed values.

The comparison between pump prototypes A and B allows for the evaluation of the effects related to the choice of a different casing technology. As described in Section 3.3, pump A has been designed with a cast iron casing that does not require running in processes; this means that radial clearances are entirely defined during the design procedure. On the contrary, prototype B is constituted by an aluminum casing, which undergoes a dedicated running in process allowing for the gearpair to produce a certain amount of wear and therefore modify the radial clearances by itself. Apart from this aspect, the two pumps are identical. On the basis of these considerations, Figure 7 shows the comparison between the two pumps in terms of the vibro-acoustic response, normalized with respect to the minimum value calculated for pump prototype A; measured efficiency is given as standard proof of the presence of cavitation. Although the overall behavior is similar, RMS values referred to pump B are considerably smaller in the range where the cavitation takes place; on the contrary, outside this range, calculated values are similar both regarding acoustic and acceleration measurements. It is therefore reasonable to assume that, since the running in process permits the gearpair to self-adjust its radial clearances through a controlled wear, it also actively contributes in reducing the intensity of the cavitation phenomenon. As underlined in Section 3.3, the higher intensity of cavitation in pump prototype A is also proved by the presence of an excessive amount of wear observed by performing endurance tests on various samples of such a prototype. From these considerations, it results that vibro-acoustic measurements performed on external gear pumps are able to quantitatively define the intensity of

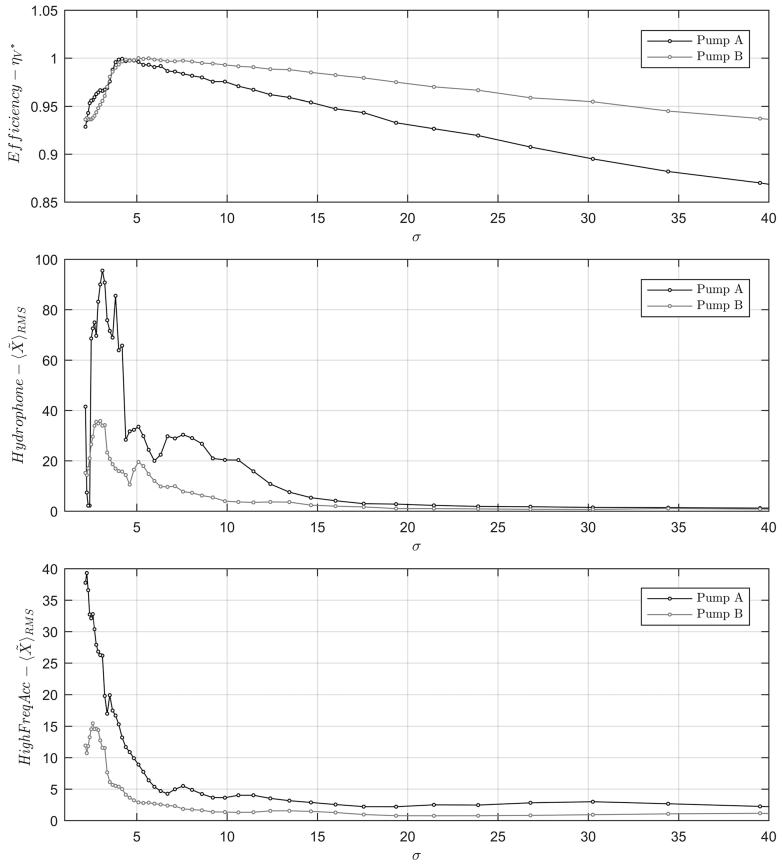

Figure 7: Comparison between pump prototypes A and B in terms of hydrophone and accelerometer response (RMS values); efficiency measurements are shown as a benchmark indicator. In each plot, symbol $\tilde{X}$ refers to the measured quantity normalized by its minimum value recorded for pump prototype A, while symbol η_V^* refers to the volumetric efficiency normalized by its maximum value.

the cavitation phenomenon, in addition to their capability to detect it in advance with respect to pressure ripple and efficiency measurements.

6 Concluding remarks

An extended experimental campaign aiming at detecting cavitation in external gear pumps by means of acceleration and acoustic measurements has been presented. With this purpose, a dedicated test rig has been instrumented with a hydrophone and a high frequency accelerometer, together with pressure ripple transducers located both on the suction and delivery chambers. Moreover, a flow meter, a tachometer and two digital pressure gauges complete the set of transducers adopted to control the pump working conditions.

In order to perform the present study, four different pump prototypes have been designed with the aim at evaluating the phenomenon under the effects of different design solutions. In particular, last prototype has been specifically designed to not be affected by cavitation throughout the entire working conditions range examined; this characteristic makes it as the reference point to assess the results. The effective presence/absence of cavitation in the four prototypes has been checked with the help of efficiency measurements and endurance tests, showing examples of various cavitation erosion marks observed.

The application of the post processing procedure has underlined the necessity of a general overview of the signals, which is achieved with the help of waterfall spectra extended to the entire measured frequency range.

This first step identifies two different regions: the low frequency one, which is mainly influenced by the mesh frequency and its harmonics, and the high frequency one, which is mainly characterized by the wideband cavitation noise.

Experimental data are filtered to enlighten the high frequency region and then RMS values of such signals are plotted with respect to the cavitation number. Comparison between pump B (cavitating) and D (not cavitating) has underlined the effective capability of the procedure in detecting the presence of the phenomenon. In particular, acceleration and acoustic measurements appeared to be highly sensitive to the phenomenon if compared to efficiency measurements as well as pressure ripple measurements. All the calculated results qualitatively reproduce the behavior usually detected in rotordynamic pumps and turbines, demonstrating that the cavitation phenomenon can be analyzed also in volumetric pumps in a similar manner. Results obtained on pump prototypes A and C (both cavitating) confirm these observations.

Influence of the oil temperature has been evaluated by reproducing the tests at three different temperature values: 60^oC, 90^oC and 120^oC. Results seem demonstrating that the temperature increasing tends to spread the development of cavitation throughout a wider speed range and, in particular, to move the fully developed cavitation condition at higher speed values. Moreover, influence of the casing technology has been evaluated: pumps made by aluminum casings resulted to be less affected by cavitation. This result may be explained by considering that aluminum casings require the pumps to undergo a dedicated running in process that allows the gearpair to self-adjust its radial clearances through a controlled wear process. This aspect seems to contribute in reducing the intensity of the cavitation phenomenon, as verified by endurance tests performed on various samples of pump prototypes A and B. The capability of the proposed procedure to capture the intensity of the phenomenon, a characteristic that efficiency curves cannot detect, can be clearly appreciated by comparing the maximum RMS values calculated for the two pump prototypes. As a consequence of this assessment, the method resulted to be able to evaluate the severity of the cavitation in gear pumps.

The proposed study therefore demonstrates that vibro-acoustic measurements coupled with a dedicated signal processing procedure are a powerful tool for the early detection of cavitation in external gear pumps and a quantitative estimation of the intensity of the phenomenon. However, it also underlines that such a phenomenon is still not completely addressed and further studies should be devoted to analyze the nature of cavitation in gear pumps in correlation with the nature of the produced signals.

References

[1] I. S. Pearsall, Acoustic detection of cavitation, Proceedings of the Institution of Mechanical Engineers 181 (1966) paper 14.

[2] P. J. McNulty, I. S. Pearsall, Cavitation inception in pumps, Journal of Fluids Engineering 104 (1) (1982) 99–104.

[3] P. A. Abbot, Cavitation detection measurements on Francis and Kaplan hydro turbines, in: R. E. A. Arndt, M. L. Billet, W. K. Blake (Eds.), Proceedings of the Third International Symposium on Cavitation, Noise and Erosion in Fluid Systems, San Francisco, CA, 1989, pp. 55–61.

[4] P. A. Abbot, C. J. Gedney, D. L. Greeley, Cavitation monitoring of two axial-flow hydroturbines using novel acoustic and vibration methods, in: Proceedings of the 13th IAHR Symposium, Vol. 1, Montreal, Canada, 1986, p. paper 23.

[5] M. Čudina, Detection of cavitation Phenomenon in a centrifugal pump using audible sound, Mechanical Systems and Signal Processing 17 (6) (2003) 1335–1347.

[6] J. Černetič, M. Čudina, Estimating uncertainty of measurements for cavitation detection in a centrifugal pump, Measurement 44 (7) (2011) 1293–1299.

[7] A. Adamkowski, A. Henke, M. Lewandowski, Resonance of torsional vibrations of centrifugal pump shafts due to cavitation erosion of pump impellers, EFA 70 (2016) 56–72.

[8] Z. Yan, J. Liu, B. Chen, X. Cheng, J. Yang, Fluid cavitation detection method with phase demodulation of ultrasonic signal, Applied Acoustics 87 (2015) 198–204.

[9] R. Azizi, B. Attaran, A. Hajnayeb, A. Ghanbarzadeh, M. Changizian, Improving accuracy of cavitation severity detection in centrifugal pumps using a hybrid feature selection technique, Measurement 108 (2017) 9–17.

[10] M. Borghi, M. Milani, F. Paltrinieri, B. Zardin, The Influence of Cavitation and Aeration on Gear Pumps and Motors Meshing Volumes Pressures, in: ASME IMECE 2006, Chicago, 2006, pp. 1–10.

[11] J. Zhou, A. Vacca, B. Manhartsgruber, A Novel Approach for the Prediction of Dynamic Features of Air Release and Absorption in Hydraulic Oils, Journal of Fluids Engineering 135 (9) (2013) 091305.

[12] J. Zhou, A. Vacca, P. Casoli, A novel approach for predicting the operation of external gear pumps under cavitating conditions, Simulation Modelling Practice and Theory 45 (2014) 35–49.

[13] E. Mucchi, G. Cremonini, S. Delvecchio, G. Dalpiaz, On the pressure ripple measurement in variable displacement vane pumps, Journal of Fluids Engineering 135 (2013) 091103.

[14] E. Mucchi, G. Dalpiaz, A. Fernandez Del Rincon, Elasto-dynamic analysis of a gear pumpPart IV: Improvement in the pressure distribution modelling, Mechanical Systems and Signal Processing (2014) 1–21.

[15] M. Battarra, E. Mucchi, G. Dalpiaz, A model for the estimation of pressure ripple in tandem gear pumps, in: ASME IDETC/CIE, 2015, p. V010T11A018; 9 pages.

[16] M. Battarra, E. Mucchi, A method for variable pressure load estimation in spur and helical gear pumps, Mechanical Systems and Signal Processing 76-77 (2016) 265–282.

[17] D. Buono, D. Siano, E. Frosina, A. Senatore, Gerotor pump cavitation monitoring and fault diagnosis using vibration analysis through the employment of auto-regressive-moving-average technique, Simulation Modelling Practice and Theory 71 (2016) 61–82.

[18] D. del Campo, R. Castilla, G. A. Raush, P. J. Gamez-Montero, E. Codina, Numerical Analysis of External Gear Pumps Including Cavitation, Journal of Fluids Engineering 134 (8) (2012) 081105.

[19] D. del Campo, R. Castilla, G. A. Raush, P. J. Gamez-Montero, E. Codina, Pressure effects on the performance of external gear pumps under cavitation, Proceedings of the Institution of Mechanical Engineers, Part C: Journal of mechanical engineering science 228 (16) (2014) 2925–2937.

[20] X. Escaler, E. Egusquiza, M. Farhat, F. Avellan, M. Coussirat, Detection of cavitation in hydraulic turbines, Mechanical Systems and Signal Processing 20 (4) (2006) 983–1007.

[21] J. P. Tullis, Hydraulics of Pipelines - Pumps, Valves, Cavitation, Transients, John Wiley & Sons, Inc., 1989.

[22] S. C. Li, Cavitation in hydraulic machinery, Imperial College Press, London, 2000.

[23] E. Mucchi, G. Dalpiaz, A. Rivola, Dynamic behavior of gear pumps: Effect of variations in operational and design parameters, Meccanica 46 (6) (2011) 1191–1212.

[24] M. Battarra, E. Mucchi, Evaluating time dependent pressure forces and torques in external gear machines by means of an analytical approach, in: INTER-NOISE, Hong Kong, 2017, pp. 6737–6748.

[25] T. Rus, M. Dular, B. Sirok, M. Hocevar, I. Kern, An Investigation of the Relationship Between Acoustic Emission, Vibration, Noise, and Cavitation Structures on a Kaplan Turbine, Journal of Fluids Engineering 129 (September) (2007) 1112.

[26] M. Čudina, J. Prezelj, Detection of cavitation in operation of kinetic pumps. Use of discrete frequency tone in audible spectra, Applied Acoustics 70 (4) (2009) 540–546.